

# Conjugated polymer-wrapped carbon nanotubes: physical properties and device applications

Widianta Gomulya, Jia Gao<sup>a</sup>, and Maria Antonietta Loi<sup>b</sup>

Zernike Institute for Advanced Materials, Nijenborgh 4, 9747 AG Groningen, The Netherlands

Received 25 July 2013

Published online (Inserted Later) – © EDP Sciences, Società Italiana di Fisica, Springer-Verlag 2013

**Abstract.** The aim of this article is to present an overview about the preparation method and physical properties of a new hybrid system consisting of single-walled carbon nanotubes (SWNTs) wrapped by conjugated polymers. The technique firstly demonstrated in 2007 has attracted great interest because of the high purity of the resulting semiconducting SWNTs and the possibility of applying them in electronic devices. Here, we will review recent progresses regarding the preparation of these nano-hybrids, their photophysical properties and application in field-effect transistors and photovoltaic devices.

## 1 Introduction

Single walled carbon nanotubes (SWNTs) are long  $sp^2$  carbon cylinders, where carbon atoms are arranged in a honeycomb lattice arrangement. Since their discovery by Iijima and Ichihashi, and Bethune et al. [1–3] in 1993 (publish independently), significant progress has been achieved both in the understanding of the physical properties and exploring possible technological applications. Notably, these quasi-one-dimensional objects have attracted tremendous scientific interest and have become one of the most investigated nano-objects in physics and material science over the last two decades.

A nanotube can be pictured as a sheet of graphene rolled into a seamless cylindrical shape. Its diameter can vary from 0.4 to 3 nm, while its length is on the scale of centimeters [4–6]; a large variety of SWNTs species can be formed by rolling the graphene sheet in different directions. The simplest way of identifying the structure of a single tube is in terms of the pair of indices  $(n, m)$  which define the chiral vector. The chiral vector is defined as:  $\mathbf{C}_h = n\mathbf{a}_1 + m\mathbf{a}_2$ , where  $(n, m)$  are lattice translational indices and  $\mathbf{a}_1$  and  $\mathbf{a}_2$  are the unit vectors of the graphene lattice in real space. The cylinder is obtained by rolling up the graphene sheet such that the two end-points of the chiral vector are superimposed. The chiral angle,  $\theta$ , is defined as the angle between the vectors  $\mathbf{C}_h$  and  $\mathbf{a}_1$ , and due to the hexagonal symmetry of the lattice this can have values in the range of  $0^\circ$  to  $30^\circ$ . The chiral angle allows classification SWNTs into achiral or chiral. Two limiting cases correspond to achiral nanotubes, when the chiral angle is  $0^\circ$ , the nanotubes are named zig-zag; and the one  $30^\circ$

are called armchair. The chiral vector also describes the circumference of the nanotube, which has a direct proportional relation with its band gap.

The electronic structure of carbon nanotubes is originated from the one of graphene. Figure 1b shows the band structure in the extended first Brillouin zone of graphene. The energy surfaces describing the valence ( $\pi$ ) and conduction ( $\pi^*$ ) states touch at six points lying at the Fermi level. The exceptional electronic properties of SWNTs are originated from the quantum confinement of the electrons normal to the nanotube axis. The periodic boundary conditions around its circumference require that the component of the momentum along the circumference is quantized ( $\mathbf{C}_h \cdot \mathbf{k}_\perp = 2\pi j$ , where  $j$  is a non-zero integer) [8]. This quantization leads to the formation of a set of discrete sub-bands for each nanotube as described by the red parallel lines in Figure 1b. The crossing of these lines with the band structure of graphene determines the electronic structure of the nanotube. If the lines pass through the Fermi point ( $K$  or  $K'$ ), the nanotube is a metal; if they do not, the nanotube is a semiconductor. In simple terms, the metallic nature of carbon nanotubes can be checked by looking at the chiral indices by the following relation  $|n - m| = 3q$ , where  $q$  is an integer. When the chiral indices are in any other relation the carbon nanotubes are semiconducting. Using a simple tight-binding model, the transition energy (band-gap) of semiconducting nanotubes  $E_g$  is described by:

$$E_g = 4\hbar v_F / 3d_{CNT} = \gamma(2R_{C-C} / d_{CNT}),$$

where  $\gamma$  is the index denoting the transition,  $R_{C-C}$  is the nearest neighbor C-C distance, and  $d$  is the nanotube diameter [9]. The density of states (DOS) of nanotubes shows sharp peaks known as van Hove singularities,

<sup>a</sup> *Current address:* Department of Chemical and Biological Engineering, Princeton University, Princeton, NJ 08544, USA

<sup>b</sup> e-mail: M.A.Loi@rug.nl

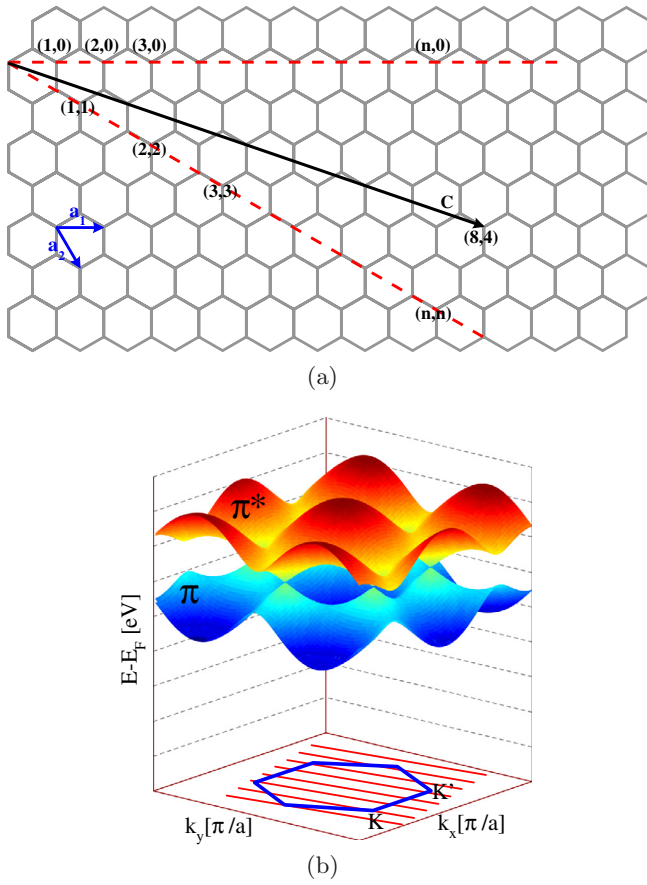


**Fig. 1.** (a) Carbon nanotubes map on graphene sheet, the primitive vectors and an example of chiral vector and chiral angle is depicted. (b) Graphene band structure. Modified from reference [7].

which are the results of the one-dimensional quantum confinement.

Because of the many progresses that have been made with the development of numerous methods to produce carbon nanotubes, they have become commercially available. Between the most common methods which can be used to obtain carbon nanotubes in sizeable quantities, we can mention: high pressure carbon monoxide (HiPCO), arc discharge (AD), pulsed laser vaporization (PLV), and chemical vapor deposition with cobalt and molybdenum oxide as catalyst (CoMoCAT) [10]. Although these techniques have been optimized for several years, there is no synthetic method giving SWNTs of one specific diameter, but the nanotubes produced with different techniques show different diameter distributions; HiPCO SWNTs: 0.7–1.3 nm; PLV SWNTs: 1–1.4 nm; AD SWNTs: 1.2–1.4 nm; CoMoCAT SWNTs: 0.7–1.2 nm. Moreover, all these methods give as product a mix of metallic and semiconducting nanotubes. SWNTs are known to have natural tendency to aggregate in large bundles and ropes as soon as they are synthesized due to van der Waals interactions between their walls.

In principle, the physical properties of individual SWNTs in an ensemble can be recognized with the aid of absorption and photoluminescence spectroscopy. However,

their tendency to form bundles obstructed early optical studies of carbon nanotubes. Only in 2002, almost one decade after the discovery of SWNTs, O'Connell et al. [11] reported the first photoluminescence spectra from SWNTs dispersed with sodium dodecyl sulfonate (SDS) in water. The most important step forward was determined by the sample preparation. Strong sonication was used in order to break the bundles, followed by ultracentrifugation to remove the remaining bundles and impurities. This method demonstrated its high effectiveness yielding to solutions with high quantities of individualized tubes. Since then, many efforts have been focused to find other techniques to disperse individual nanotubes and to sort them in different species and chiralities. Between the methods used we can distinguish the attempts to functionalize covalently the walls of SWNTs from the one that use a non-covalent functionalization [12]. The last are generally preferred because the desire to leave the physical properties of the nanotubes as much unchanged [13]. One of the methods that utilize non-covalent interaction is DNA-assisted dispersion [14]. In contrast to the surfactants, which have not specific interaction with carbon nanotube species, DNA was found to have a preferential interaction with certain tube species [15].

In the early study of carbon nanotubes, conjugated polymer such as poly(p-phenylenevinylene-co-2,5-dioctyloxy-m-phenylenevinylene) (PmPV) has been reported to interact with multi-walled carbon nanotubes [16]. However, only recently conjugated polymers have been used for the dispersion of SWNTs. Nish et al. [17] reported for the first time that conjugated polymers are able to interact selectively with certain semiconducting nanotube species solubilizing them. Poly(9,9-dioctylfluorene-2,7-diyl) (PFO) is exceptional in enabling highly efficient de-bundling of semiconducting-SWNTs (s-SWNTs), especially for tubes of diameter around  $\sim 1$  nm and large chiral angle ( $>24^\circ$ ).

The large efforts in searching suitable techniques for the separation and sorting of SWNTs are determined not only by the need to have isolated SWNTs to study their physical properties but also by the desire to apply SWNTs in the fabrication of electronic devices. One of the main attraction of carbon nanotubes is the ballistic transport and the consequent very high mobility along the tubes [18]. The electrical properties of carbon nanotubes have been extensively explored since the demonstration of the first single carbon nanotube field-effect transistors (SWNT-FETs) which showed excellent performances with hole mobility  $20 \text{ cm}^2/\text{Vs}$  and on/off ratio  $10^5$  [19]. However, due to the difficulties in single SWNTs device fabrication, the technological interest has been hampered. Later, the use of SWNTs dispersed with surfactants open a new way to cheap fabrication techniques for nanotubes random network transistors [20,21]. Nevertheless, the lack of the nanotubes selectivity makes the on/off ratio of these devices generally limited. The separation of semiconducting nanotubes by polymer wrapping opens the opportunity for low cost processing and high performing electronic and optoelectronic devices based on SWNTs. While the

application in field effect transistors is the most natural because of their excellent mobility, SWNTs can also be incorporated in organic photovoltaic devices to improve the charge mobility [22]. Later reports show SWNTs capabilities as acceptor material in combination mostly with conjugated polymers [23], or as a donor materials to harvest solar energy [24,25].

In this work we review recent progresses made in the separation and sorting of SWNTs by their electrical properties using polymer wrapping, and the application of this hybrid nanomaterials in electronics and optoelectronics. In the first part, we will discuss the different polymers that have been used to separate nanotubes so far, analyzing their selectivity for semiconducting tubes. Secondly, we summarize reports, which show the advantages of polymer wrapping to investigate the photophysics of SWNTs. At the end the implementation of single wall carbon nanotubes in field-effect transistor and solar cell devices will be reviewed.

## 2 Polymer for selective sorting SWNTs

Pristine SWNTs exhibit great tendency to aggregate and form bundles due to  $\pi$ - $\pi$  interactions between their walls. These bundles may contain nanotubes with various diameter, chirality and electrical properties, which largely limit their application in electronics or optoelectronics. It is, thus, highly desirable to develop effective methods to extract specific nanotubes from the ensemble. One of the most widely used strategies is to disperse SWNTs in solution with the aid of surfactants or other molecules. Sodium dodecyl sulphate (SDS) [11], sodium dodecylbenzene sulphonate (SDBS) [26], sodium cholate [27], and many others bile salts have been proven effective in dispersing SWNTs in aqueous solution. These molecules have both a hydrophobic group (tail), which orients in the direction of the nanotube wall and a hydrophilic group (head), which is in contact with water. Because of the nature of their interaction with the SWNTs, these surfactants do not show any selectivity to specific species of nanotubes. This separation becomes less useful especially in device application because of mixture of electrical properties, i.e., one third of the SWNTs are metallic and two thirds are semiconducting. Density gradient ultracentrifugation (DGU) is able to overcome these obstacles by isolating the semiconducting nanotubes from the metallic ones [27]. By using mixtures of two surfactants in different ratio followed by ultracentrifugation in a density gradient medium, carbon nanotubes can be sorted by diameter and band gap due to their density difference. The result is a multi-layer colored solutions, colors of which are deriving by the different band gaps of the SWNTs species. The use of non-linear DGU enables optimizations of the nanotubes separation to obtain single chirality tubes [28]. This technique is already applied for commercial purpose separating both semiconducting and metallic Arc Discharge- or Plasma Torch- SWNTs with 99% and 98% purity, respectively [25,29]. Other methods for sorting SWNTs such as DNA wrapping [30], agarose gel [31], and gel chromatography [32] have also been reported recently.

$\pi$ -conjugated polymers have been shown to be efficient dispersant for the solubilization of SWNTs. Among the large family of conjugated polymers, polyfluorene and its co-polymers show unique selectivity toward specific kinds of semiconducting nanotubes. The sample preparation procedure is relatively easy compared with other techniques such as DGU or gel chromatography. The technique involves a simple sonication and ultracentrifugation of polymer-SWNTs mixture. The selectivity mechanism has been first discussed based on molecular dynamics simulations, putting forward the hypothesis that the  $\pi$ - $\pi$  stacking of the polymer backbone and nanotube walls surface dominates the binding energy between the polymer and the carbon nanotubes [17]. This simulation also suggests that the polymers backbone align parallel to the wall of the nanotubes. However, the effectiveness of selective sorting of SWNTs is not only determined by the structure of the macromolecules, but also by the solvent used [33,34]. PFO shows the most pronounced selectivity in "bad" solvents such as toluene or xylene. When "good" solvents such as tetrahydrofuran (THF) or dichlorobenzene (oDCB) are used, the selectivity of PFO towards semiconducting carbon nanotubes is jeopardized. In the case of chloroform, dispersed SWNTs showed the highest absorbance intensity, while no photoluminescence was observed [33]. Such results suggest a close relationship between the solubility of the polymer in a certain solvent with its selectivity towards semiconducting SWNTs.

Our group investigated the mechanism of polymer-SWNTs interaction by combining spectroscopic experiments with molecular dynamics and quantum chemical calculations [35]. In our case, the molecular dynamic simulation included the solvent (toluene) providing a more realistic system respect to previously reported calculations. Moreover, we succeeded in removing the excess polymer present in the solution of PFO wrapped semiconducting SWNTs and observed the modified photoluminescence of the wrapped polymers. By comparing the experimental results with calculation, we conclude that the alkyl tails of neighboring polymer chains zip and align through van der Waals interactions, following the zigzag motifs of the nanotube wall (Fig. 2a). The solvent, toluene in this case, favors the helical wrapping of the polymer chains on the wall of SWNTs, as seen in the molecular dynamic simulations where the calculated potential energy is lower compare to the aligned one (Fig. 2b).

Besides PFO, many other fluorene-based conjugated polymers have been tested on their capacity of sorting SWNTs in the last 5 years. Figure 3 summarizes the structures of the polymers, which have shown selectivity towards SWNTs with different chiralities or diameters. Recently, we have elucidated the influence of the side chains structure on the effectiveness of polyfluorene derivatives of sorting semiconducting carbon nanotubes [36]. Poly(9,9-di-(N,N-dimethylaminopropylfluorenyl)-2,7-diyl) (PFDMA) with amine-end side chain and [(N,N,N-trimethylammonium)-propyl]-(2,7-fluorene dibromide) (PFAB) with ammonium salts side chains have been investigated in water-based

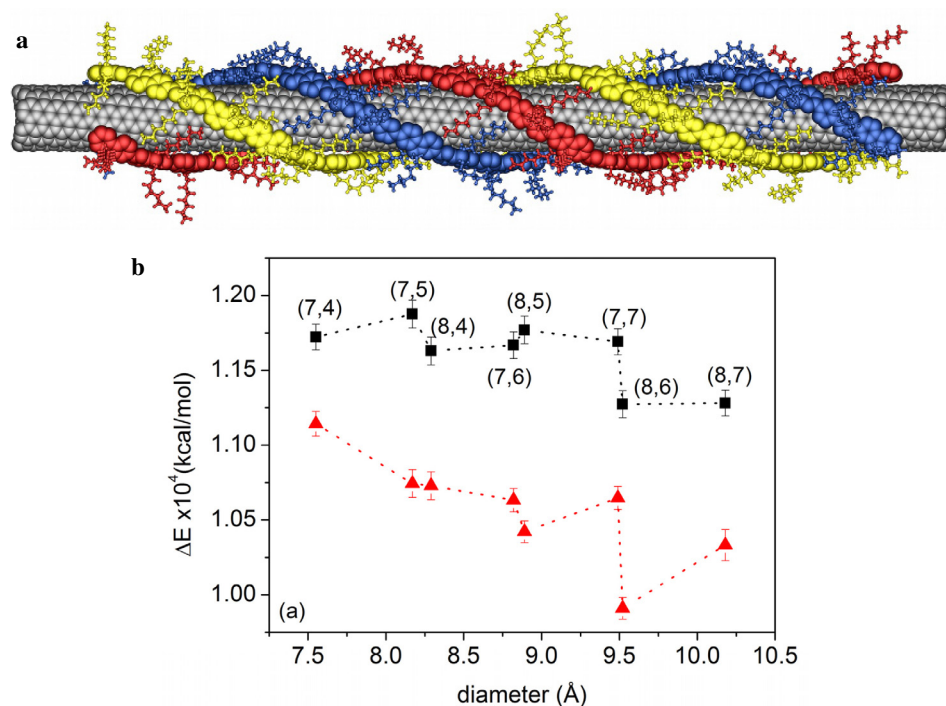


**Fig. 2.** (a) PFO wrapped nanotubes in helical geometry. Here one tube is wrapped with three PFO chains (represented as blue, red, and yellow structures). (b) Binding energy of PFO-wrapped SWNT in toluene, for chains aligned to the tube axis (black) and rolling up as helices (red) as a function of diameter (reprinted with permission from Ref. [35]. Copyright 2011, American Chemical Society).

solutions. The selectivity of these two polymers toward SWNTs is inferior to that of PFO, likely due to the less efficient zipping of the short side chains on the nanotubes walls compared to that of the octyl chains of PFO. However, it is necessary to underline that the results are barely comparable because of the solvent dissimilarity and the role of the solvent in the process. Our finding is consistent with the report that polyfluorene with shorter side chain such as poly[9,9-dihexylfluorenyl-2,7-diyl] (PFH) [17,37] is less effective in selective sorting SWNTs and interacts with different set of SWNTs species due to lack of zipping mechanism.

Fluorene-based copolymers have also attracted great interest for sorting SWNTs. In general, these copolymers show selectivity towards HiPCO carbon nanotubes with larger diameter. For example, poly[(9,9-dioctylfluorenyl-2,7-diyl)-alt-co-(1,4-benzo-2,1',3-thiadiazole)] (PFO-BT) was reported to be selective towards SWNTs with diameter  $\sim 1.05$  nm, this seems to be triggered by the thiazole group since poly[(9,9-dioctylfluorenyl-2,7-diyl)-co-(1,4-phenylene)] (PFO-P) shows poor selectivity in the same diameter range [17]. Poly(9,9-didodecylfluorene-2,7-diyl-alt-anthracene-1,5-diyl) (PF12-A) shows selectivity on nanotubes with larger diameter, and is claimed that this large diameter selectivity is due to the anthracene unit [39].

Recently, we have demonstrated for the first time that large diameter ( $>1.2$  nm) semiconducting carbon nanotubes can be efficiently separated and individualized using long alkyl chain polyfluorene derivatives [37]. These polymers (with alkyl chains larger than octyl) exhibit affinity for a number of semiconducting SWNT chiralities contained both in small diameter nanotubes (diameter between 0.8–1.2 nm), as well as in large diameter

tubes (diameter of about 1.4 nm). In both cases, polyfluorenes with long side chains allow obtaining dispersions of highly individualized semiconducting SWNT with very high concentration and containing SWNT species that could not be selected previously. Molecular dynamics simulations showed that the long alkyl tails on polyfluorenes provide a stronger binding to the nanotube wall and a variety of wrapping geometries that allow more nanotube species to be suspended. These results are consistent with a more efficient solubilization, a less specific selection of nanotube chiralities and a large range of nanotube diameter selected as the length of the alkyl chains increases, as observed experimentally. The high quality of the sample, in terms of individualization of SWNTs and low defect induced with the processing in the SWNT walls is demonstrated by the long photoluminescence lifetimes and the elevated photoluminescence yield measured especially for the polyfluorene derivatives with dodecyl alkyl chains-wrapped SWNTs (PF12). The high quality and density of SWNTs is confirmed by the outstanding performances of the field effect transistors fabricated with the SWNTs dispersions. The device results will be discussed in detail in next section.

A degradable PFO copolymer, poly[(9,9-dioctylfluorenyl-2,7-diyl)-alt-co-1,1,2,2-tetramethyldisilane] with selectivity for SWNTs with a diameter range from 1 to 1.2 nm and large chiral angles was presented by Wang et al. [40]. This copolymer has disilane groups, which are degradable under hydrofluoric acid (HF). The possibility of removing the polymer-wrapped around the SWNTs is very attractive for device application. However, the selectivity of this polymer is not satisfactory. The purity of semiconducting SWNTs is low, proven by evidence of metallic tubes in the absorption spectra and the low

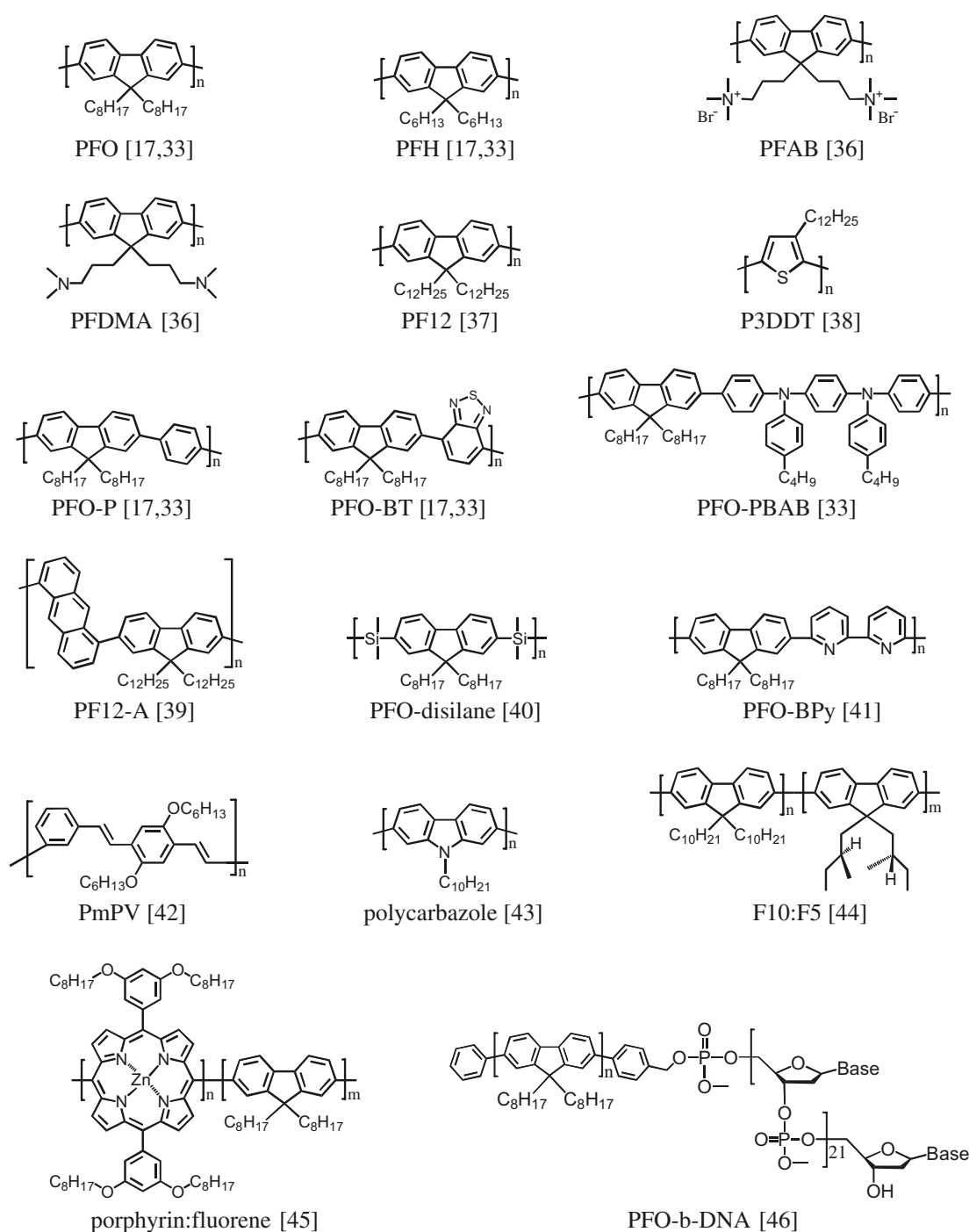


**Fig. 3.** Structure of the polymers that have been demonstrated to sort selectively SWNTs in terms of diameter or chiral angle.

on/off ratio of the field effect transistors. Another interesting copolymer is poly(9,9-dioctylfluorenyl-2,7-diyl and bipyridine) (PFO-BPy). In contrast to other fluorene copolymers, this polymer can extract almost single chirality small diameter nanotubes (97% of (6,5)-SWNTs) using p-xylene as solvent [41]. This result opens the opportunity for extracting single chirality s-SWNTs by using polymer wrapping.

Block copolymers have also attracted interest for nanotubes separation, Ozawa et al. [44] reported the design

of chiral block-copolymer. Solutions containing different chirality and diameter of SWNTs from polydisperse to near monodisperse, are obtained by tuning the ratio of the blocks of the polymer decylfluorene and 9,9-bis[(S)-(+)-2-methylbutyl]fluorene (F10:F5).

The block-copolymer porphyrin-octofluorene shows similar selectivity to PFO with the exception of its ability of selecting the (9,5) nanotubes [45]. Several polymers without fluorene units have also been reported to show selectivity towards SWNTs. PmPV shows the best

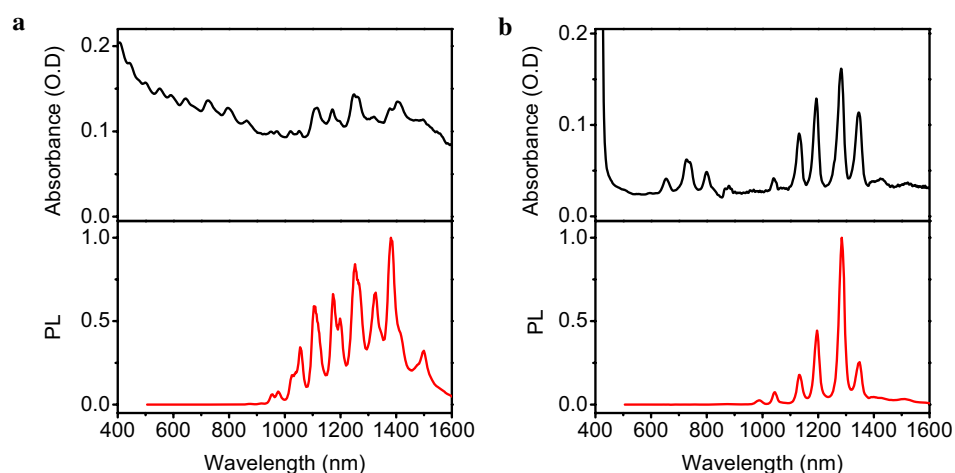


**Fig. 4.** Absorption and photoluminescence of SWNTs dispersed in (a) SDBS/D<sub>2</sub>O and (b) PFO/toluene.

selectivity to nanotubes with diameter around 1.2 nm [42]. However, the stability of this polymer-wrapped nanotubes is very low. Dispersed SWNTs precipitate in couple of weeks and even faster (in couple of hours) under UV-visible illumination.

Polycarbazoles show selectivity complementary to that of polyfluorene, i.e. *s*-SWNTs with low chiral angles are selected [43]. A very recent report from Lee et al. [38] demonstrates that polythiophenes with long alkyl side chains can also act as efficient nanotube dispersant. The best polythiophene derivative reported by the authors is regioregular poly(3-dodecylthiophene) (rr-P3DDT).

Single-stranded DNA (ss-DNA) because of its structural features has been explored very early for the separation of SWNTs [12,47]. A recent study by Tu et al. [15] shows that ss-DNA has great selectivity for single chirality nanotubes, using specific sequence of DNA, the sorting of particular (n,m)-SWNTs species was demonstrated. Recently, we report a new utilization of DNA in combination with PFO. With the aim to exploit the potentiality of PFO in recognizing semiconducting carbon nanotubes, with the addressability of DNA, a DNA block copolymer (PFO-b-DNA) was synthesized [46]. This block co-polymer soluble in water shows selectivity slightly worse than the one obtained from PFO in toluene solution, which indicates that the wrapping process is dominated by the PFO part. The molecular dynamics simulations also confirmed the preferential interaction with the PFO block. After the successful separation of semiconducting SWNTs, the pairing of the single strand DNA sequence was used to self-assembly the nanotubes in device structures, by using thiols-DNA pair (c-DNA) attached to the transistor source-drain electrodes to address the self-assembly of the SWNTs. The device performance obtained with these self-assembled SWNTs will be discussed in details below.

### 3 Photophysics of SWNTs

The photophysical properties of SWNTs have attracted great interest during the last decades due to their unique characteristics. Being one-dimensional system, SWNTs

show van Hove singularities in their density of states [9]. They have strong charge confinement and relatively strongly bound exciton, which manifest themselves with sharp optical absorption and photoluminescence peaks in the near infrared region. However, these unique properties are obstructed when SWNTs are spatially very close one to each other, i.e., when they bundle in triangular structures through van der Waals interaction. The absorption spectrum of SWNTs bundles exhibits severe inhomogeneous broadening as the result of overlapping between the energy states of different nanotube structures. Fluorescence also could not be observed from bundles because photoexcitations are completely quenched, as a consequence of large exciton energy transfer to semiconducting tubes with narrower energy gaps or quenching to adjacent metallic tubes [48–50].

The photophysical properties of SWNTs dispersed in aqueous solution have been extensively studied in the last decade [11,51]. However, it has been reported recently that SWNTs dispersed by surfactant molecules remain in small bundles instead of being individually dispersed [52]. The photoluminescence quantum yield in these samples is generally limited to the range of 0.01%–0.1% [11], which is much smaller than what has been observed in suspended SWNTs in air (8%) [26]. Polyfluorene-wrapped SWNTs in organic solvent are in this respect superior to water-surfactant dispersions, since they show quantum yields as high as 1.5% [17]. High quality semiconducting nanotube samples produced in this manner make this technique becomes important for the study of the fundamental properties of SWNTs and their interaction with other species.

Figure 4 shows the absorption and the photoluminescence spectra of HiPCO SWNTs (diameter of 0.8–1.2 nm) dispersed with sodium dodecylbenzene sulphonate (SDBS) and with PFO. The characteristic absorption peaks in the wavelength range from 1000 to 1600 nm and 600 to 900 nm correspond to the first and second van Hove transitions ( $E_{11}$ ,  $E_{22}$ ) of the semiconducting SWNTs species, while the absorption of metallic tubes is in the range of 500–600 nm. In the case of SWNTs in SDBS aqueous solution (Fig. 4a), the presence of both semiconducting and metallic SWNTs is evident from the

absorption spectrum. The PL spectrum also indicates the presence of more than 10 types of semiconducting SWNTs in the final dispersion.

The absorption and photoluminescence spectra of SWNTs dispersion in PFO/toluene solution are shown in Figure 4b. Here, at wavelengths higher than 1000 nm are the  $E_{11}$  transitions of five different SWNTs species, which according to the assignment performed based on the empirical Kataura plot are the (7,5), (7,6), (8,6), (8,7), and (9,7) [9,17]. The SWNTs dispersion in PFO/toluene shows much lower absorption background and lower full width at half maximum (FWHM) of the single absorption peaks respect to the one displayed by the dispersion with SDBS in aqueous solution. The photoluminescence lifetime of the SWNTs, which is the dynamics of the “bright” exciton in (7,5) tubes is shown in Figure 5. Polymer wrapped SWNTs show longer decay time (38 ps) than the same nanotubes separated by surfactants (22 ps). However, the very dissimilar dielectric constant of the two solvents does not allow to draw a conclusion on the degree of isolation or tube quality [53]. Another merit of the polymer wrapping separation technique is that the polymer does not affect the properties of the SWNTs in the near infrared region since the polymer has a much larger band-gap [54]. This allows studying the photophysical properties of carbon nanotubes without any interference.

A matrix of photoluminescence excitation spectra (PLE) of PFO wrapped SWNTs in toluene is shown in Figure 6 [55]. The satellite luminescence of the highly isolated nanotubes, which are labeled as  $(E_{11} + G)$  and  $(E_{11} + G')$  are clearly shown in the PLE map. This photoluminescence originated from the interaction of the excitons with G-phonons, which are in plane lattice vibrations. In the figure, the  $E_{12}$  and  $E_{21}$  transitions are also evident. These weak transitions originate from the excitons with dipole moments cross-polarized respect to the tube axis and can be observed by perpendicularly polarized optical measurements. Furthermore, these results show the existence of dark excitonic states as indicated by extremely weak luminescence at the de-excitation energy equal to  $(E_{11} - G)$ . These emissions correspond to coupling between K-point phonons and dipole-forbidden dark excitons. Murakami et al. [56] have also studied the existence of the dark excitonic states and found them 140 meV below the  $E_{11}$  transition. The existence of dark excitons in carbon nanotubes was also proven measuring the splitting of the  $E_{11}$  energy band upon application of an external magnetic field, known as Aharonov-Bohm effect [57]. By using polymer-wrapped SWNTs, a very well resolved exciton splitting could be observed.

SWNTs wrapped with PFO have been adopted for the investigation of the exciton dynamics with time-resolved spectroscopy. Miyauchi et al. [58] calculated the exciton radiative life time based on the PL decay and the photoluminescence yields of the nanotubes and obtained the value of  $\sim 3$ –10 ns. The same authors also evaluated the coherence length of exciton in SWNTs and found that it is in order of 10 nm, independent of the nanotubes diameter. Koyama et al. [50] demonstrated the possibility of energy

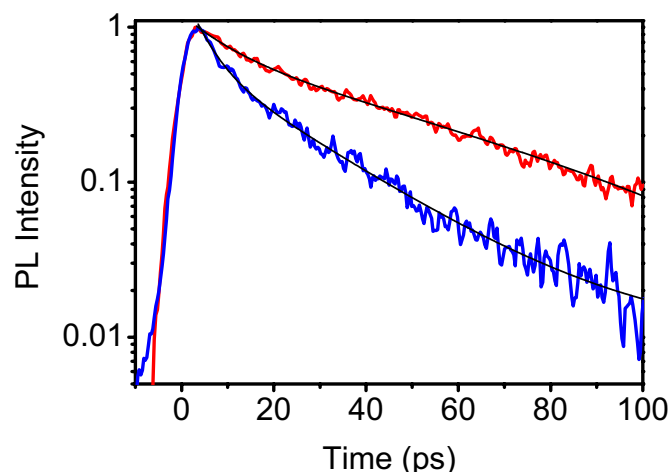


**Fig. 5.** Time resolved photoluminescence of (7,5) SWNTs dispersed in SDBS/D<sub>2</sub>O (blue) and PFO/toluene (red).

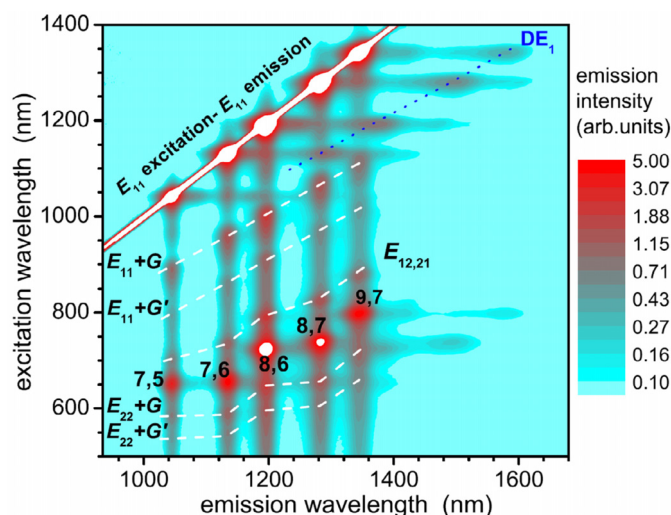


**Fig. 6.** PLE map of HiPCO nanotubes dispersed in PFO/toluene showing five emitting (n,m) species with large helical angles (reprinted figure with permission from Ref. [55]. Copyright 2008 by the American Physical Society).

transfer between adjacent bundled nanotubes. These experimental results show that the lifetime of SWNTs become shorter as their energy gap decreases. Similar results were obtained in experiments performed by our group, where we observed bi-exponential decay times for bundled nanotubes, and single exponential decay when the SWNTs are well dispersed [36]. Significant increase of the lifetime from (6,5) tubes to (7,5) tubes was also observed.

The non-radiative decay of excitons in SWNTs is another important topic due to the very low fluorescence quantum yield. Matsuda et al. [59] reported a systematic study on the decay of excitons by hole-doping of polymer-wrapped SWNTs and concluded that the exciton decay is dominated by phonon emission (phonon-assisted indirect exciton ionization).

**Table 1.** Comparison of transistor performance.

SWNTs preparation procedure	Channel length ( $\mu\text{m}$ )	Mobility ( $\text{cm}^2/\text{Vs}$ )	On/off ratio	Carrier type
DGU/Self-assembly [61]	2	10	$10^4$	ambipolar
DGU [21]	200	1.5	$>10^4$	p-type
Dielectrophoresis [68]	5	123–9*	$10\text{--}10^4*$	p-type
SDS/SC wrapped [70]	25	10	up to $10^7$	p-type
PFO/Dielectrophoresis [71]	0.5	–	$10^4\text{--}10^5$	p-type
PFO wrapped/network [73]	5	2	$10^5$	p-type
PFO wrapped/network [74]	5	3 (electron)	$>10^6$	ambipolar
DNA-PFO wrapped/Self-assembly [46]	0.3	–	$5 \times 10^4$	ambipolar
Degradable PFO wrapped [40]	20	5.2	$1.5 \times 10^4$	p-type
CVD [66]	5–50	1200–200*	$10\text{--}10^4*$	p-type
PECVD [75]	2–10	8	$>10^5$	ambipolar
P3DDT wrapped/network [38]	1.5	12	$>10^6$	p-type

\* post treatment using electrical breakdown process.

## 4 Polymer-wrapped SWNTs for device application

### 4.1 Polymer-wrapped SWNTs for transistor application

Field-effect transistors (FETs) are considered to be the building blocks of modern microelectronic technology. The major function of FETs is to modulate the current flow between source and drain electrodes that is channeled by a semiconducting material, by applying a bias voltage to a third electrode called gate electrode. Silicon has been the dominant semiconductor since the second half of the 20th century. However, silicon based transistors are now approaching their limits in performances [60]. Nowadays, transistors based on silicon with channel length of 20 nm are produced and this appears as being very close to the limit of downscaling possibilities. s-SWNTs have shown great potential as conducting channel for field-effect transistors (FETs) [61–63]. The performance of s-SWNTs based FETs have proven to be superior to that of silicon transistors [6]. The protocols used for SWNTs device fabrication can be generally placed in two categories. In the first category, s-SWNTs are grown on a substrate by either catalytic chemical vapor deposition (CVD) method at high temperature ( $\sim 900$  °C) or using plasma enhanced CVD method at low temperature ( $\sim 450$  °C), then the electrodes are patterned by electron beam lithography [6,64–67]. In the second category, pristine SWNTs are dispersed in aqueous or organic solution and then deposited by cheap solution-based methods on the substrate with pre-patterned electrodes to form random networks of nanotubes [21,68–70]. This process scheme allows for large area device preparation, which is certainly more suitable for further device integration and low cost electronics.

Recently, solution-processed assembly techniques for the alignment of s-SWNTs, such as evaporation self-assembly [61], dielectrophoresis [68,71], Langmuir-Blodgett assembly [72], DNA-assisted self-assembly [46] have shown great promise for the improvement of device performance compared to that of the random network nanotubes. However, many of the device characteristics

show low on/off ratio, especially in the short channel length devices, due to presence of residual metallic tube in the solution. Post-treatments, such as electrical breakdown has been used to improve the on/off ratio at the expense of carrier mobility [66,68]. Table 1 compares to date device performance obtained with different preparation procedure. Obviously, polymer-wrapped semiconducting carbon nanotubes are one of the promising candidates for high performances solution-processed field-effect transistors [73].

So far, there have been a couple of reports on the preparation of s-SWNTs dispersion by using conjugated polymers to make electronic devices. Lee et al. [38] prepared s-SWNTs dispersion with regioregular poly(3-dodecylthiophene) (rr-P3DDT) and they obtained FET devices with mobility as high as  $12 \text{ cm}^2/\text{Vs}$  and on/off  $10^6$ . Vijayaraghavan et al. [71] demonstrated transistor made by single chirality nanotubes that are selected by PFO. An increment of the on/off ratio up to one order of magnitude in multiple parallel-assembled nanotubes devices compared to that in single tubes devices is observed in their experiment. From these experiments it also appears that the removal of the polymer is essential to achieve high performing devices. The residual polymers can form tunneling barriers both between the metal electrodes and the nanotubes and between nanotubes, and induces charge scattering along the nanotubes. IZard et al. [73] showed that filtration can effectively separate the s-SWNTs from the excess polymers, obtaining devices with hole mobility as high as  $2 \text{ cm}^2/\text{Vs}$  with on/off ratio  $\sim 10^5$ . Bindl et al. [76,77] presented a method with multiple centrifugation steps to remove excess polymer from s-SWNTs solution.

Our group adopted this polymer removal method, by applying two ultracentrifugation steps, which has the advantage of being less time consuming and provide high extraction yield of s-SWNTs by avoiding iterative re-dispersion [74]. Using this highly concentrated samples we obtained high performance ambipolar transistors with on/off ratio higher than  $10^6$  for both holes and electrons (Fig. 7a); and mobility values as high as  $3 \text{ cm}^2/\text{Vs}$  (calculated from the linear regime of the transfer curve

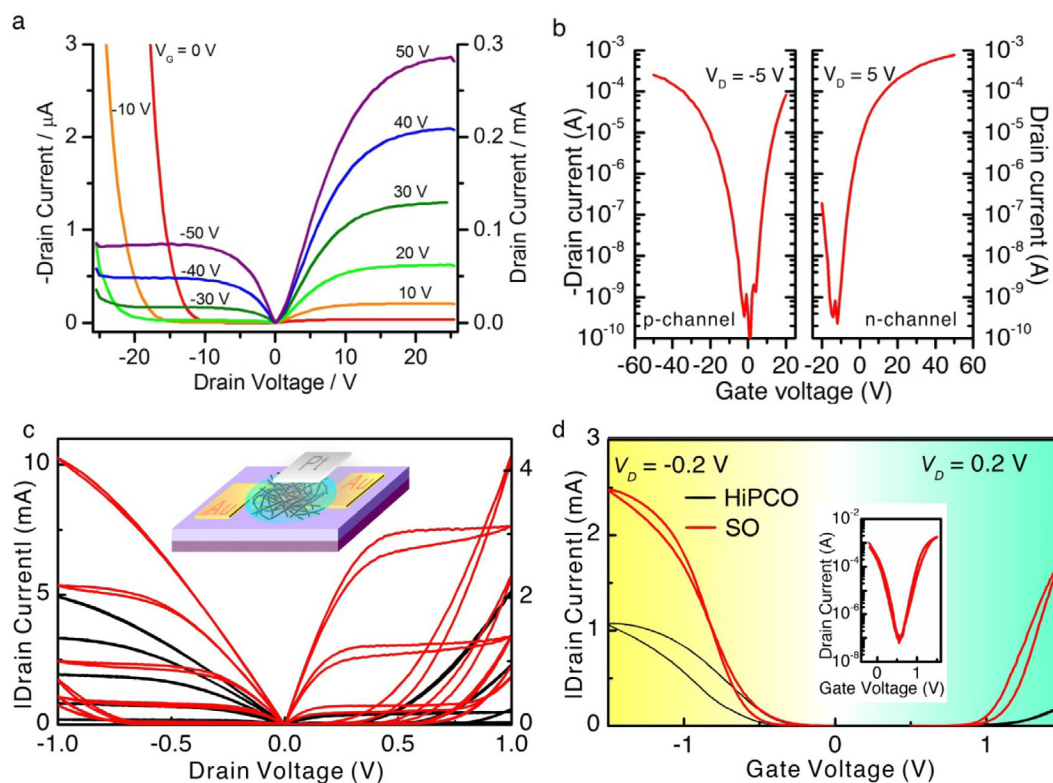


**Fig. 7.** (a) Output characteristics of the CoMoCAT s-SWNT FET. (b) p-channel (left) and n-channel (right) transfer characteristics of the device with on/off ratio  $>10^6$  (reprinted with permission from Ref. [74]. Copyright 2012, WILEY-VCH Verlag GmbH & Co. KGaA, Weinheim). (c) Output characteristics of ion-gel gated transistors (inset) made from HiPCO SWNTs (black curves) and SO SWNTs (red curves). (d) The comparison of the transfer characteristics of the corresponding devices for both p-channel and n-channel operations. The inset shows the logarithmic scale plot of the transfer curve of the transistor made from SO SWNTs with on/off ratio  $>10^4$  (reprinted with permission from Ref. [37]. Copyright 2013, WILEY-VCH Verlag GmbH & Co. KGaA, Weinheim).

in Fig. 7b). These electron mobility values are among the highest reported for devices made with solution processed s-SWNT. In most of SWNTs transistor fabricated from water-based solutions reported in literature, the carbon nanotubes devices show p-type characteristics. The lack of n-type behavior, is commonly due to increasing of work function of the electrode with exposure in air, which results in a better injection for holes [78] and electrochemical interaction between adsorbed molecules (water and/or oxygen) and s-SWNTs, which could induce an electron transfer from SWNTs the molecules [79].

As mentioned previously, selection of large diameter SWNTs was achieved by using long alkyl chain polyfluorene derivatives. FET devices, with an ionic gel gate and as active elements dodecylalkyl-chain-polyfluorene-derivatives-wrapped - HiPCO and - SO s-SWNT [37], exhibit high on/off ratio exceeding more than  $10^4$  and  $10^5$  at  $V_D = 0.2$  V. For HiPCO s-SWNT FETs the hole and electron mobilities are about  $5.7$   $\text{cm}^2/\text{V s}$  and  $3.6$   $\text{cm}^2/\text{V s}$ , respectively. While SO s-SWNT FETs with higher hole ( $14.3$   $\text{cm}^2/\text{V s}$ ) and electron ( $16.4$   $\text{cm}^2/\text{V s}$ ) mobilities are obtained [37]. The output and transfer curves showing the comparison between HiPCO and SO tubes are shown in Figures 7c and 7d.

The possibility to assemble SWNTs in specific positions on a substrate is one of the holy grail of SWNTs electronics, because could allow to make single s-SWNTs devices by self-assembly. Recently, we have demonstrated the application of DNA block copolymer (PFO-b-DNA) for the dispersion and self-assembly of SWNTs (Fig. 8a) [46]. This composite powerfully combines all the advantages of the individual polymer in separating and selecting s-SWNTs, and of DNA. The hydrophobic segments of this copolymer, PFO, interact with s-SWNTs while the hydrophilic segments, single stranded DNA (ss-DNA) remains available for straightforward duplex pairing with its complementary part (cDNA). The schematic presentation of how this PFO-DNA copolymer works for the dispersion and self-assembly of s-SWNTs is shown in Figures 8b–8d. The photoluminescence spectra of the dispersed HiPCO SWNTs with different dispersant are shown in Figure 8e, indicate the good selectivity achieved with this copolymer in water.

We further prepared field effect transistors by self-assembly of the dispersed SWNTs with PFO-b-DNA and achieved device yield as high as 98%. Pre-patterned Au electrodes were firstly functionalized with a mixed monolayer complementary thiol-modified ODN (cDNA) and

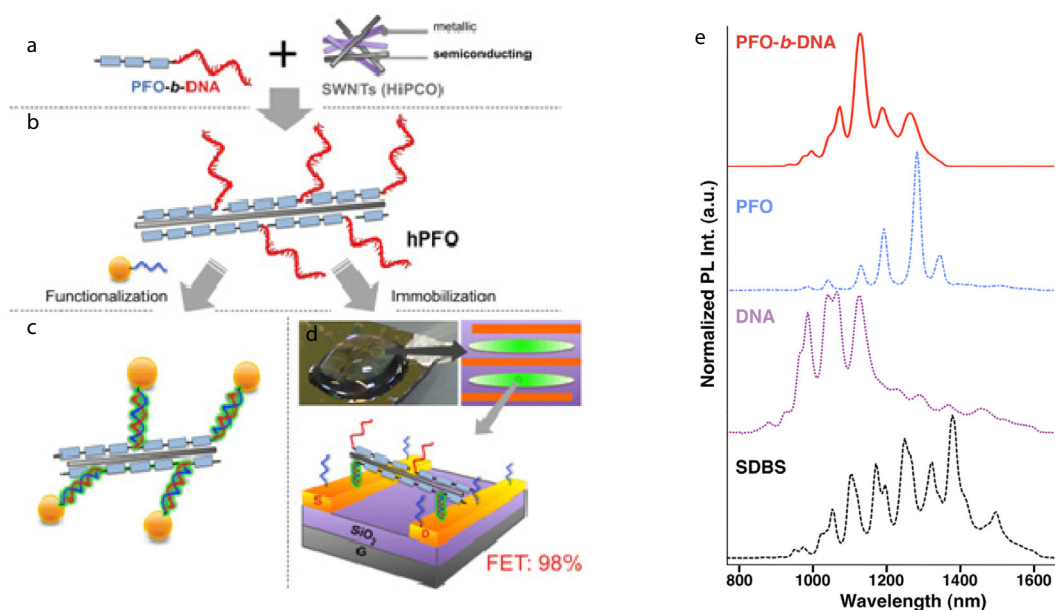


**Fig. 8.** (a) DNA block copolymer (PFO-*b*-DNA), (b) s-SWNTs species wrapped by PFO block, (c) hybridization of cDNA-modified (blue) Au-nanoparticles (yellow spheres) and ss-DNA, (d) immobilized SWNTs on defined cDNA surfaces, such as electrodes of field-effect transistors (FETs), (e) normalized photoluminescence of HiPCO carbon nanotubes wrapped by PFO-*b*-DNA, PFO, ss-DNA, and SDBS (reprinted with permission from Ref. [46]. Copyright 2011, WILEY-VCH Verlag GmbH & Co. KGaA, Weinheim).

mercaptohexanol (MCH). Despite of the continuous exposure to air and water, 80% of the working devices show ambipolar characteristics and on/off ratio up to  $5 \times 10^4$  (channel length 300 nm). This work opens a new approach for nanotubes alignment into devices with a very simple fabrication procedure.

#### 4.2 Polymer-wrapped SWNTs for solar cell application

Nowadays, solar cell production is mostly based on single- and multi-crystalline Si heterojunctions, which exhibit power conversion efficiency (PCE) up to  $\sim 25\%$ . However, due to the complex production techniques and high fabrication costs, many alternatives are currently being investigated. One of the prime choice to produce cheap devices is organic materials [80]. A typical bulk heterojunction organic solar cell comprises a mixture of a  $\pi$ -conjugated polymer and a fullerene derivative. Figure 9a shows the energy levels of some of the most used active materials, namely poly(3-hexylthiophene) (P3HT), and the fullerene derivative PCBM. The energy offset between the LUMO of the donor polymer and the LUMO of the acceptor molecule is sufficiently large to provide the energy needed to separate the tightly bound electron-hole pair. The dissociated carriers, electrons and holes move to the cathode through PCBM layer and to the anode through conjugated polymer, respectively. The highest PCE in organic solar cells reached  $\sim 10\%$  so far [81]. The limited carrier mobility and narrow absorption spectra in the visible range of the fullerene derivatives can be considered one of the limiting factors. The high charge mobility of semiconducting

SWNTs makes them interesting candidates to be implemented in this class of solar cells [82].

SWNTs have been adopted as acceptors in the early reports of organic photovoltaics in replacement of PCBM. Performance improvements were expected considering the higher mobility of the s-SWNTs respect to fullerenes. Nevertheless, the formation of a type II heterojunction has not been verified in these systems even if many photophysical and electrical experiments were conducted to confirm the possibility of charge extraction from polymer to nanotubes [83–85]. PCE of 0.52% was reported for solar cells using P3HT and SWNTs as active layer [86]. Recently, an increased power conversion efficiency up to 0.72% ascribed to the removal of metallic nanotubes has been achieved [87]. By wrapping the s-SWNTs walls with P3HT as illustrated in Figure 9b, two main advantages are obtained, preventing the nanotubes aggregation, and increasing the charge extraction. However, the PCE for these devices are still much lower than that obtained for optimized P3HT/PCBM cells  $\sim 6.5\%$  [88]. Recently, Ham et al. [89] have predicted based on the calculation of the effective area of one single nanotube, that the maximum efficiency reachable for P3HT/SWNTs cells is about 3.8%, indicating that the design and fabrication of the devices can be further optimized.

s-SWNTs, interestingly, can act either as donor or as acceptor depending on the material that is combined together with. In combination with P3HT small diameter s-SWNTs can act as acceptor (Fig. 9a), while when they are combined with C60 or PCBM, they can also act as donors as illustrated in Figure 9c. It should be noted that

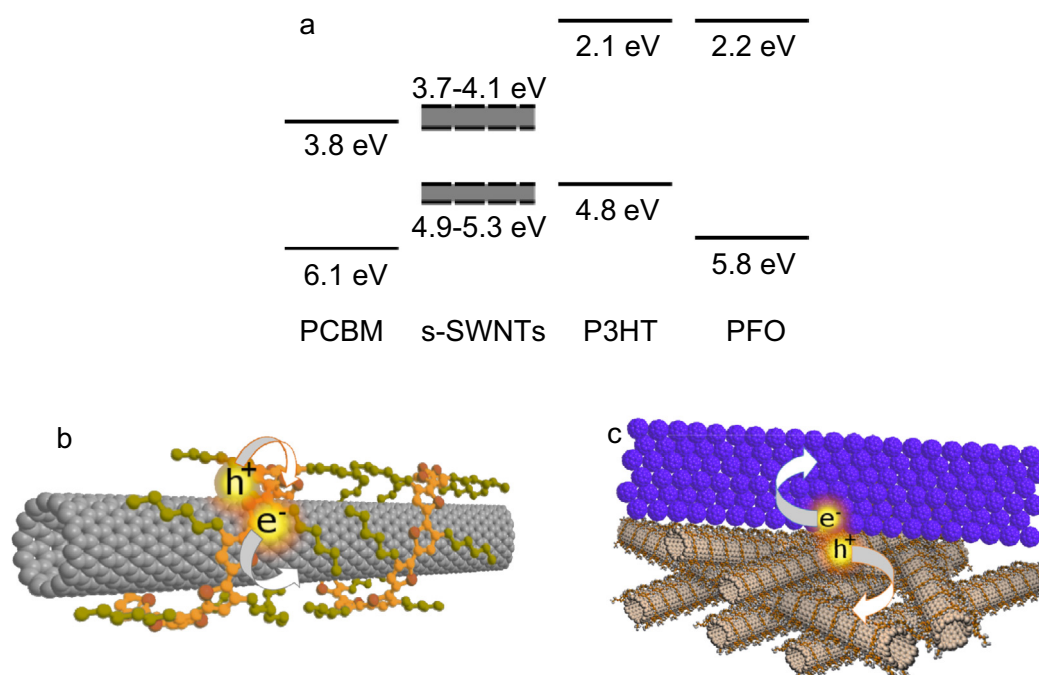


**Fig. 9.** (a) Energy levels alignment for PCBM, s-SWNTs, P3HT, and PFO; (b) type II heterojunction formed by P3HT wrapped s-SWNTs (modified from Ref. [83]); (c) s-SWNTs/PCBM heterojunction (modified from Ref. [77]).

from their energy level alignment, PFO-wrapped SWNTs cannot be used as efficient heterojunction for solar cells.

The group of Arnold demonstrated the fabrication of photodetectors in which the heterojunction is formed by C60 with PFO-wrapped nanotubes [90]. The devices show internal quantum efficiency (IQE) up to 44%, which indicates the efficient exciton dissociation at this interface. These devices also work as photovoltaic cells and the PCE reaches  $\sim 0.6\%$ ; which is much higher than that of the mixed-SWNTs/C60 devices with only 0.001% efficiency [77]. A recent report shows bulk heterojunction cells with 18.3% external quantum efficiency (EQE) in the NIR region by adding PCBM to the s-SWNTs layers [24]. Further studies have demonstrated EQE reaching 43% in the NIR region and PCE up to 1% for s-SWNT active layer thickness  $< 5$  nm [91]. Other researchers reported 0.46% PCE using a P3DDT-SWNTs/C60 heterojunction. Also in this work, very thin layer of s-SWNTs are used due to short exciton diffusion length [92].

Investigations about the charge extraction were conducted by Strano group by fabricating single chirality carbon nanotubes photovoltaic cell and studying the influence of multiple species of s-SWNTs in the active layer [93]. The authors found that the different nanotubes species can act as the electron/hole traps that can reduce devices performance. Here charge hopping between adjacent nanotubes is considered, against the expectation that charges should move along the nanotube axis with their high mobility.

Bindl et al. [94] examined the influence of the polymer residue (PFO in this case) on the device efficiency and found an hindered transport. The devices performances increase by decreasing the amount of polymer residue,

proving the role of the excess polymer as a barrier in the charge extraction especially when the polymer does not form a type II heterojunction with the s-SWNT. Nevertheless, the charge transfer is also limited by the short exciton diffusion length, calculated as  $\sim 3$  nm in SWNTs film.

Further studies are needed in the future to improve performances of solar cell based on semiconducting carbon nanotubes, only the next years will demonstrate if they have a real interest for conversion of solar energy in electricity.

## 5 Summary

Conjugated polymer-wrapped SWNTs have been proven as a very efficient and easy technique to individualize nanotubes with high degree of selectivity for semiconducting species. SWNTs dispersions obtained in this way have demonstrated to be in many respects superior to water based surfactant dispersions. Their absorption show very low background and very sharp peaks corresponding to the absorption of the individual semiconducting species. Photoluminescence spectroscopy shows high quantum efficiency (1.5%) and excitation lifetime as long as 38 ps. These characteristics make of polymer wrapping the ideal preparation method to study the physical properties of carbon nanotubes.

The ability of the polymer wrapping technique to separate efficiently semiconducting from metallic tubes opens possibilities for large-scale semiconducting nanotubes production for solution processable electronic devices such as transistor and solar cell. The transistor performance

obtained with polymer-wrapped s-SWNTs are superior to the one obtained with deposition methods such as PECVD or density gradient samples. Hole and electron mobilities in the order of several to tens  $\text{cm}^2/\text{Vs}$  with on/off ratio up to  $10^7$  have been obtained. Moreover, has been shown that by using PFO-ss-DNA block copolymer it is possible to self-assemble s-SWNTs in predetermined positions of a substrate.

While the application of SWNTs in solar cells is in its infancy, it has been shown that they can be used as alternative material for electron acceptor, as well as a donor material. The efficiency obtained so far is still very low (maximum efficiency reported 1.4%) and more efforts are necessary to achieve higher power conversion efficiency and understand if s-SWNTs can play a role in solar energy conversion

The authors acknowledge Technologistichting STW and NanoSci-ERA (a consortium of national funding organizations within European Research Area) for the funding of the project Nano-Hybrids for Photonic Devices (NaPhoD) and the University of Groningen for the Bernoulli scholarship of W.G. We thank F. van der Horst and A. Kamp for the technical supports.

## References

1. S. Iijima, T. Ichihashi, *Nature* **363**, 603 (1993)
2. D.S. Bethune, C.H. Klang, M.S. de Vries, G. Gorman, R. Savoy, J. Vazquez, R. Beyers, *Nature* **363**, 605 (1993)
3. M. Monthieux, V.L. Kuznetsov, *Carbon* **44**, 1621 (2006)
4. N. Wang, Z.K. Tang, G.D. Li, J.S. Chen, *Nature* **408**, 50 (2000)
5. Q.-H. Yang, S. Bai, J.-L. Sauvajol, J.-B. Bai, *Adv. Mater.* **15**, 792 (2003)
6. P. Avouris, J. Appenzeller, R. Martel, S.J. Wind, *Proc. IEEE* **91**, 1772 (2003)
7. P. Avouris, Z. Chen, V. Perebeinos, *Nat. Nanotechnol.* **2**, 605 (2007)
8. R. Saito, G. Dresselhaus, M.S. Dresselhaus, *Physical Properties of Carbon Nanotubes* (Imperial College Press, 1998), pp. 37–47
9. R. Saito, G. Dresselhaus, M.S. Dresselhaus, *Phys. Rev. B* **61**, 2981 (2000)
10. M.H. Rummeli, P. Ayala, T. Pichler, in *Carbon Nanotubes and Related Structures*, edited by D.M. Guldi, Nazariortín (Wiley-VCH Verlag GmbH & Co. KGaA, 2010), pp. 1–21
11. M.J. O'Connell, S.M. Bachilo, C.B. Huffman, V.C. Moore, M.S. Strano, E.H. Haroz, K.L. Rialon, P.J. Boul, W.H. Noon, C. Kittrell, J. Ma, R.H. Hauge, R.B. Weisman, R.E. Smalley, *Science* **297**, 593 (2002)
12. M.C. Hersam, *Nat. Nanotechnol.* **3**, 387 (2008)
13. R. Martel, *ACS Nano* **2**, 2195 (2008)
14. M. Zheng, A. Jagota, E.D. Semke, B.A. Diner, R.S. Mclean, S.R. Lustig, R.E. Richardson, N.G. Tassi, *Nat. Mater.* **2**, 338 (2003)
15. X. Tu, S. Manohar, A. Jagota, M. Zheng, *Nature* **460**, 250 (2009)
16. S.A. Curran, P.M. Ajayan, W.J. Blau, D.L. Carroll, J.N. Coleman, A.B. Dalton, A.P. Davey, A. Drury, B. McCarthy, S. Maier, A. Strevens, *Adv. Mater.* **10**, 1091 (1998)
17. A. Nish, J.-Y. Hwang, J. Doig, R.J. Nicholas, *Nat. Nanotechnol.* **2**, 640 (2007)
18. C.T. White, T.N. Todorov, *Nature* **393**, 240 (1998)
19. R. Martel, T. Schmidt, H.R. Shea, T. Hertel, P. Avouris, *Appl. Phys. Lett.* **73**, 2447 (1998)
20. E. Adam, C.M. Aguirre, L. Marty, B.C. St-Antoine, F. Meunier, P. Desjardins, D. Ménard, R. Martel, *Nano Lett.* **8**, 2351 (2008)
21. C.W. Lee, C.-H. Weng, L. Wei, Y. Chen, M.B. Chan-Park, C.-H. Tsai, K.-C. Leou, C.H.P. Poa, J. Wang, L.-J. Li, *J. Phys. Chem. C* **112**, 12089 (2008)
22. S. Cataldo, P. Salice, E. Menna, B. Pignataro, *Energy Environ. Sci.* **5**, 5919 (2012)
23. E. Kymakis, G.A.J. Amaratunga, *Appl. Phys. Lett.* **80**, 112 (2002)
24. D.J. Bindl, A.S. Brewer, M.S. Arnold, *Nano Res.* **4**, 1174 (2011)
25. Y. Li, S. Kodama, T. Kaneko, R. Hatakeyama, *Appl. Phys. Express* **4**, 065101 (2011)
26. D.A. Tsyboulski, J.-D.R. Rocha, S.M. Bachilo, L. Cagnet, R.B. Weisman, *Nano Lett.* **7**, 3080 (2007)
27. M.S. Arnold, A.A. Green, J.F. Hulvat, S.I. Stupp, M.C. Hersam, *Nat. Nanotechnol.* **1**, 60 (2006)
28. S. Ghosh, S.M. Bachilo, R.B. Weisman, *Nat. Nanotechnol.* **5**, 443 (2010)
29. L. Huang, H. Zhang, B. Wu, Y. Liu, D. Wei, J. Chen, Y. Xue, G. Yu, H. Kajiura, Y. Li, *J. Phys. Chem. C* **114**, 12095 (2010)
30. S.N. Kim, Z. Kuang, J.G. Grote, B.L. Farmer, R.R. Naik, *Nano Lett.* **8**, 4415 (2008)
31. T. Tanaka, H. Jin, Y. Miyata, S. Fujii, H. Suga, Y. Naitoh, T. Minari, T. Miyadera, K. Tsukagoshi, H. Kataura, *Nano Lett.* **9**, 1497 (2009)
32. H. Liu, D. Nishide, T. Tanaka, H. Kataura, *Nat. Commun.* **2**, 309 (2011)
33. J.-Y. Hwang, A. Nish, J. Doig, S. Douven, C.-W. Chen, L.-C. Chen, R.J. Nicholas, *J. Am. Chem. Soc.* **130**, 3543 (2008)
34. F. Jakubka, S.P. Schießl, S. Martin, J.M. Englert, F. Hauke, A. Hirsch, J. Zaumseil, *ACS Macro Lett.* **1**, 815 (2012)
35. J. Gao, M.A. Loi, E.J.F. de Carvalho, M.C. dos Santos, *ACS Nano* **5**, 3993 (2011)
36. J. Gao, M. Kwak, J. Wildeman, A. Herrmann, M.A. Loi, *Carbon* **49**, 333 (2011)
37. W. Gomulya, G.D. Costanzo, E.J.F. de Carvalho, S.Z. Bisri, V. Derenskyi, M. Fritsch, N. Fröhlich, S. Allard, P. Gordiichuk, A. Herrmann, S.J. Marrink, M.C. dos Santos, U. Scherf, M.A. Loi, *Adv. Mater.* **25**, 2948 (2013)
38. H.W. Lee, Y. Yoon, S. Park, J.H. Oh, S. Hong, L.S. Liyanage, H. Wang, S. Morishita, N. Patil, Y.J. Park, J.J. Park, A. Spakowitz, G. Galli, F. Gygi, P.H.-S. Wong, J.B.-H. Tok, J.M. Kim, Z. Bao, *Nat. Commun.* **2**, 541 (2011)
39. N. Berton, F. Lemasson, J. Tittmann, N. Stürzl, F. Hennrich, M.M. Kappes, M. Mayor, *Chem. Mater.* **23**, 2237 (2011)
40. W.Z. Wang, W.F. Li, X.Y. Pan, C.M. Li, L. Li, Y.G. Mu, J.A. Rogers, M.B. Chan-Park, *Adv. Funct. Mater.* **21**, 1643 (2011)
41. H. Ozawa, N. Ide, T. Fujigaya, Y. Niidome, N. Nakashima, *Chem. Lett.* **40**, 239 (2011)

42. W. Yi, A. Malkovskiy, Q. Chu, A.P. Sokolov, M.L. Colon, M. Meador, Y. Pang, *J. Phys. Chem. B* **112**, 12263 (2008)
43. F.A. Lemasson, T. Strunk, P. Gerstel, F. Hennrich, S. Lebedkin, C. Barner-Kowollik, W. Wenzel, M.M. Kappes, M. Mayor, *J. Am. Chem. Soc.* **133**, 652 (2010)
44. H. Ozawa, T. Fujigaya, Y. Niidome, N. Hotta, M. Fujiki, N. Nakashima, *J. Am. Chem. Soc.* **133**, 2651 (2011)
45. H. Ozawa, X. Yi, T. Fujigaya, Y. Niidome, T. Asano, N. Nakashima, *J. Am. Chem. Soc.* **133**, 14771 (2011)
46. M. Kwak, J. Gao, D.K. Prusty, A.J. Musser, V.A. Markov, N. Tombros, M.C.A. Stuart, W.R. Browne, E.J. Boekema, G. ten Brinke, H.T. Jonkman, B.J. van Wees, M.A. Loi, A. Herrmann, *Angew. Chem. Int. Ed.* **50**, 3206 (2011)
47. X. Tu, M. Zheng, *Nano Res.* **1**, 185 (2008)
48. O.N. Torrens, D.E. Milkie, M. Zheng, J.M. Kikkawa, *Nano Lett.* **6**, 2864 (2006)
49. T. Koyama, K. Asaka, N. Hikosaka, H. Kishida, Y. Saito, A. Nakamura, *J. Phys. Chem. Lett.* **2**, 127 (2011)
50. T. Koyama, Y. Miyata, Y. Asada, H. Shinohara, H. Kataura, A. Nakamura, *J. Phys. Chem. Lett.* **1**, 3243 (2010)
51. R.B. Weisman, S.M. Bachilo, *Nano Lett.* **3**, 1235 (2003)
52. J. Crochet, M. Clemens, T. Hertel, *J. Am. Chem. Soc.* **129**, 8058 (2007)
53. J. Gao, W. Gomulya, M.A. Loi, *Chem. Phys.* **413**, 35 (2013)
54. A. Nish, J.-Y. Hwang, J. Doig, R.J. Nicholas, *Nanotechnology* **19**, 095603 (2008)
55. S. Lebedkin, F. Hennrich, O. Kiowski, M.M. Kappes, *Phys. Rev. B* **77**, 165429 (2008)
56. Y. Murakami, B. Lu, S. Kazaoui, N. Minami, T. Okubo, S. Maruyama, *Phys. Rev. B* **79**, 195407 (2009)
57. S. Takeyama, H. Suzuki, H. Yokoi, Y. Murakami, S. Maruyama, *Phys. Rev. B* **83**, 235405 (2011)
58. Y. Miyauchi, H. Hirori, K. Matsuda, Y. Kanemitsu, *Phys. Rev. B* **80**, 081410 (2009)
59. K. Matsuda, Y. Miyauchi, T. Sakashita, Y. Kanemitsu, *Phys. Rev. B* **81**, 033409 (2010)
60. D.J. Frank, R.H. Dennard, E. Nowak, P.M. Solomon, Y. Taur, H.-S.P. Wong, *Proc. IEEE* **89**, 259 (2001)
61. M. Engel, J.P. Small, M. Steiner, M. Freitag, A.A. Green, M.C. Hersam, P. Avouris, *ACS Nano* **2**, 2445 (2008)
62. X. Duan, C. Niu, V. Sahi, J. Chen, J.W. Parce, S. Empedocles, J.L. Goldman, *Nature* **425**, 274 (2003)
63. P.L. McEuen, M.S. Fuhrer, Hongkun Park, *IEEE Trans. Nanotechnol.* **1**, 78 (2002)
64. Z. Zhang, S. Wang, Z. Wang, L. Ding, T. Pei, Z. Hu, X. Liang, Q. Chen, Y. Li, L.-M. Peng, *ACS Nano* **3**, 3781 (2009)
65. S. Wang, Z. Zhang, L. Ding, X. Liang, J. Shen, H. Xu, Q. Chen, R. Cui, Y. Li, L. Peng, *Adv. Mater.* **20**, 3258 (2008)
66. S.J. Kang, C. Kocabas, T. Ozel, M. Shim, N. Pimparkar, M.A. Alam, S.V. Rotkin, J.A. Rogers, *Nat. Nanotechnol.* **2**, 230 (2007)
67. W.J. Yu, B.R. Kang, I.H. Lee, Y. Min, Y.H. Lee, *Adv. Mater.* **21**, 4821 (2009)
68. P. Stokes, E. Silbar, Y.M. Zayas, S.I. Khondaker, *Appl. Phys. Lett.* **94**, 113104 (2009)
69. S. Fujii, T. Tanaka, Y. Miyata, H. Suga, Y. Naitoh, T. Minari, T. Miyadera, K. Tsukagoshi, H. Kataura, *Appl. Phys. Express* **2**, 071601 (2009)
70. C.W. Lee, X. Han, F. Chen, J. Wei, Y. Chen, M.B. Chan-Park, L. Li, *Adv. Mater.* **22**, 1278 (2010)
71. A. Vijayaraghavan, F. Hennrich, N. Stürzl, M. Engel, M. Ganzhorn, M. Oron-Carl, C.W. Marquardt, S. Dehm, S. Lebedkin, M.M. Kappes, R. Krupke, *ACS Nano* **4**, 2748 (2010)
72. X. Li, L. Zhang, X. Wang, I. Shimoyama, X. Sun, W.-S. Seo, H. Dai, *J. Am. Chem. Soc.* **129**, 4890 (2007)
73. N. Izard, S. Kazaoui, K. Hata, T. Okazaki, T. Saito, S. Iijima, N. Minami, *Appl. Phys. Lett.* **92**, 243112 (2008)
74. S.Z. Bisri, J. Gao, V. Derenskyi, W. Gomulya, I. Iezhokin, P. Gordiichuk, A. Herrmann, M.A. Loi, *Adv. Mater.* **24**, 6147 (2012)
75. W.J. Yu, U.J. Kim, B.R. Kang, I.H. Lee, E.-H. Lee, Y.H. Lee, *Nano Lett.* **9**, 1401 (2009)
76. D.J. Bindl, N.S. Safron, M.S. Arnold, *ACS Nano* **4**, 5657 (2010)
77. D.J. Bindl, M.-Y. Wu, F.C. Prehn, M.S. Arnold, *Nano Lett.* **11**, 455 (2010)
78. V. Derycke, R. Martel, J. Appenzeller, P. Avouris, *Appl. Phys. Lett.* **80**, 2773 (2002)
79. C.M. Aguirre, P.L. Levesque, M. Paillet, F. Lapointe, B.C. St-Antoine, P. Desjardins, R. Martel, *Adv. Mater.* **21**, 3087 (2009)
80. C.J. Brabec, S. Gowrisanker, J.J.M. Halls, D. Laird, S. Jia, S.P. Williams, *Adv. Mater.* **22**, 3839 (2010)
81. M.A. Green, K. Emery, Y. Hishikawa, W. Warta, E.D. Dunlop, *Prog. Photovoltaics Res. Appl.* **20**, 12 (2012)
82. H. Zhu, J. Wei, K. Wang, D. Wu, *Sol. Energy Mater. Sol. Cells* **93**, 1461 (2009)
83. T. Schuettfort, A. Nish, R.J. Nicholas, *Nano Lett.* **9**, 3871 (2009)
84. C.-K. Chang, J.-Y. Hwang, W.-J. Lai, C.-W. Chen, C.-I. Huang, K.-H. Chen, L.-C. Chen, *J. Phys. Chem. C* **114**, 10932 (2010)
85. A.J. Ferguson, J.L. Blackburn, J.M. Holt, N. Kopidakis, R.C. Tenent, T.M. Barnes, M.J. Heben, G. Rumbles, *J. Phys. Chem. Lett.* **1**, 2406 (2010)
86. M. Lanzi, L. Paganin, D. Caretti, *Polym. J.* **49**, 4942 (2008)
87. S. Ren, M. Bernardi, R.R. Lunt, V. Bulovic, J.C. Grossman, S. Gradečak, *Nano Lett.* **11**, 5316 (2011)
88. M.T. Dang, L. Hirsch, G. Wantz, *Adv. Mater.* **23**, 3597 (2011)
89. M.-H. Ham, G.L.C. Paulus, C.Y. Lee, C. Song, K. Kalantar-Zadeh, W. Choi, J.-H. Han, M.S. Strano, *ACS Nano* **4**, 6251 (2010)
90. M.S. Arnold, J.D. Zimmerman, C.K. Renshaw, X. Xu, R.R. Lunt, C.M. Austin, S.R. Forrest, *Nano Lett.* **9**, 3354 (2009)
91. M.J. Shea, M.S. Arnold, *Appl. Phys. Lett.* **102**, 243101 (2013)
92. M.P. Ramuz, M. Vosgueritchian, P. Wei, C. Wang, Y. Gao, Y. Wu, Y. Chen, Z. Bao, *ACS Nano* **6**, 10384 (2012)
93. R.M. Jain, R. Howden, K. Tvrđy, S. Shimizu, A.J. Hilmer, T.P. McNicholas, K.K. Gleason, M.S. Strano, *Adv. Mater.* **24**, 4436 (2012).
94. D.J. Bindl, M.J. Shea, M.S. Arnold, *Chem. Phys.* **413**, 29 (2013)